Journal of Photochemistry and Photobiology A: Chemistry 140 (2001) 53–66

Journal of Photochemistry and Photobiology A:Chemistry

www.elsevier.nl/locate/jphotochem

New insights about diazonium salts as cationic photoinitiators

Uwe Müller [a,*], Andreas Utterodt [a], Wolfgang Mörke [b], Bernward Deubzer [c], Christian Herzig [c]

[a] *Institut für Organische Chemie, Martin-Luther-Universität, Halle-Wittenberg, Geusaer Straße, D-06217 Merseburg, Germany*

[b] *Institut für Analytik und Umweltchemie, Martin-Luther-Universität, Halle-Wittenberg, Geusaer Straße, D-06217 Merseburg, Germany*

[c] *Wacker-Chemie GmbH, Johannes-Heß-Str. 24, D-84489 Burghausen, Germany*

Received 7 November 2000; accepted 11 January 2001

Abstract

4-Hexyloxysubstituted diazonium salts with complex anions are thermostable compounds in several solvents (dioxane: 12 days; 1,2-dichloroethane: 410 days; 40°C; salt as SbF_6^-).

These salts initiate efficiently the photocrosslinking of vinyl ethers and epoxides. Interestingly, oxygen influences the efficiency of this cationic process. EPR-experiments prove that radicals possess a key function for the production of the initiating species. α-Ether radicals induce a secondary radical-induced cation formation. Such reactions are always possible if E_{red} of the onium salt is lower than −1 V. Oxygen inhibits this radical-induced cation formation. On the other hand, the decay of peroxides results in a branched radical reaction. The reaction rate is faster under air with respect to inert conditions.

The high thermostability of the used salt decreases by addition of a small amount of monomer. A bimolecular dediazoniation mechanism explains the observed effects. This mechanism produces directly initiating cationic species, which start the cationic polymerization.

The monomer and its byproducts are the cause of the poor thermal stability of the diazonium salts and not the own thermal instability of the salt used.

Keywords: Diazonium salts; Cationic photocrosslinking; Kinetics; Siloxane derivatives

1. Introduction

Aromatic diazonium salts with anions of low nucleophilicity [1] have received remarkable attention as the first efficient photoinitiators for cationic polymerization. The poor thermal stability of diazonium salts often limits their use as photoinitiators for cationic systems. Nevertheless, diazonium salts possess sufficient thermal stability in diazomicro films and printing plates [2] over several months or years.

4-Alkyloxysubstituted diazonium salts with complex anions like BF_4^-, PF_6^-, SbF_6^- and $B(C_6F_5)_4^-$ are thermally stable compounds in several solvents. The measured half-lifetimes of the hexafluoroantimonates in solution can be greater than 12 days at 40°C. They strongly depend on the solvent used (dioxane: 12 days; dimethoxyethane (DME): 17 days; acetonitrile: 360 days; methylene chloride: 360 days; 1,2-dichloroethane: 410 days). Moreover, the UV-absorption of these salts ($\lambda_{max} \approx 315$ nm; $\varepsilon \approx 27{,}000\,l\,mol^{-1}\,cm^{-1}$) overlaps sufficiently with the emission line of excimer lamps ($\lambda = 308$ nm). Additionally, no absorption of diffuse daylight and a high photosensitivity ($\Phi \approx 0.4$) characterize these onium salts. As a result, the photosensitivity of these diazonium salts is better in comparison to the sensibility of alkoxy-substituted diphenyliodonium salts (λ_{max} (methanol) ≈ 245 nm, shoulder < 340 nm; $\varepsilon_{max} < 16{,}000\,l\,mol^{-1}\,cm^{-1}$; $\Phi \approx 0.3$–0.2 [3], see also [4,5]) and alkoxysubstituted triphenyl sulfonium salts (λ_{max} (methanol) ≈ 260 nm, shoulder < 340 nm; $\varepsilon_{max} < 16{,}000\,l\,mol^{-1}\,cm^{-1}$; $\Phi \approx 0.2$ [6,7]), which were often used as photoinitiators for cationic photocrosslinking [6–11].

Both photosensitivity and the match between absorption maxima and emission line of excimer lamps argue for the use of diazonium salts as photoinitiators. Nevertheless, diazonium salts are known as relative unstable compounds. The contradiction in the thermal stability in several applications was the purpose to reexamine again the cationic photopolymerization of epoxides and vinyl ether derivatives using diazonium salts as photoinitiators; see Scheme 1.

* Corresponding author. Present address: Kompetenzzentrum Holz GmbH, St.-Peter-Straße 25, A-4021 Linz, Austria.
Tel.: +43-732-6911-4084; fax: +43-732-6911-4086.
E-mail address: uwe.mueller@uar.at (U. Müller).

1010-6030/01/$ – see front matter
PII: S1010-6030(01)00382-3

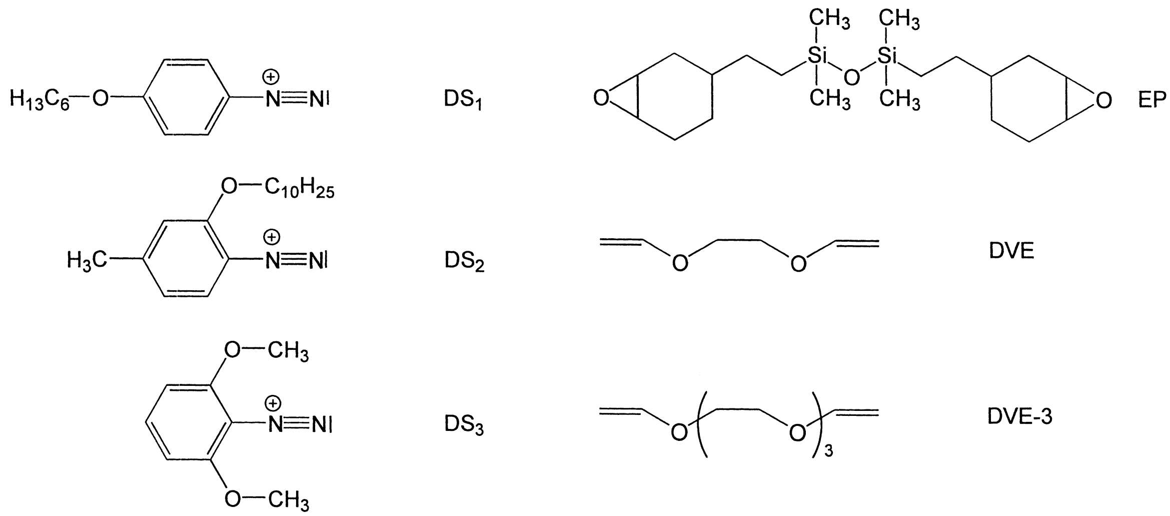

Scheme 1.

2. Experimental

2.1. Materials

Chemical structures are summarized in Scheme 1. The diazonium salts DS_1, DS_2, and DS_3 were prepared from the corresponding aniline derivatives by suspension diazotization in a concentrated aqueous $NaNO_2$ solution. The preparation of all complex salts takes place in a similar manner. Modification of the diazotization conditions helped in the isolation of the salts. The following procedures were successful in order to synthesize the salts DS_1, DS_2, and DS_3, respectively.

2.1.1. Hexafluorophosphate of DS_1

5.8 g of 4-hexyloxyaniline (Aldrich) were stirred in 18 ml concentrated hydrochloric acid and diazotized with 2.1 g $NaNO_2$ at 5°C. The hexafluorophosphate of DS_1 was prepared from the chloride solution by precipitation of the salt by addition of 5 ml HPF_6 (60%, Aldrich). The salts obtained were first washed with water and finally with pentane until all water was removed. Afterwards, the product was dried over P_4O_{10} under reduced pressure. The purification was carried out by dissolving in a small amount of acetonitrile, filtration and slow adding dry peroxide free ether at 10°C. F_P = 46–57°C (decomposition temperature = 100°C); yield = 87%.

2.1.2. Hexafluorophosphate of DS_2

2.6 g of 2-decyloxy-4-methylaniline (prepared from 2-decyloxy-4-methyl nitrobenzene) were diazotized with 0.7 g $NaNO_2$ at 5°C in a mixture of 6 ml concentrated hydrochloric acid and 10 ml methanol. Additionally, 2 ml HPF_6 (60%) were added. The salt precipitates after addition of the double volume of ice water. The salt was purified as described above. F_P = 92–94°C (decomposition temperature > 110°C); yield = 49%.

2.1.3. Hexafluorophosphate of DS_3

0.2 g of 2,6-dimethoxyaniline (prepared from 2,6-dimethoxy nitrobenzene — Aldrich) were diazotized with 0.09 g $NaNO_2$ at 5°C in a mixture of 0.3 ml concentrated hydrochloric acid and 1 ml water. Additionally, 0.2 ml HPF_6 (60%) were added. The salt was isolated and purified as described above. F_P = 165–175°C (under decomposition); yield = 67%.

2.1.4. Tetrafluoroborate of DS_1

3 g of the aniline were stirred in 5 ml concentrated HCl, 1 ml water and 4 ml methanol and diazotized with a concentrated solution of 1.1 g $NaNO_2$ at 10°C. The salt was prepared from the chloride solution by precipitation after addition of 3.2 ml HBF_4 (50%, Fluka). The tetrafluoroborate could be isolated by addition of the double volume of ice water. The purification takes place as described above. F_P = 53–58°C (under decomposition); yield = 62%.

2.1.5. Tetra(pentafluorophenyl)borate of DS_1

0.58 g of aniline were stirred in 0.9 ml concentrated HCl, 5 ml water and 10 ml methanol and diazotized with a concentrated solution of 0.21 g $NaNO_2$ at 10°C. The salt was obtained from the chloride solution by precipitation of the salt by addition of 2.15 g $Na[B(C_6F_5)_4]$ (UD FC/MO Feinchemikalien Metallorganyle, Merseburg) dissolved in 50 ml methanol. The product obtained was washed with water and dried over P_4O_{10} under reduced pressure. The waxy salt melts under decomposition (F_P > 60°C); yield = 68%.

2.1.6. Hexafluoroantimonate of DS_1

5.8 g of the aniline were stirred in 9 ml concentrated HCl, 10 ml water and 20 ml methanol and diazotized with a concentrated solution of 2.1 g $NaNO_2$ at 10°C. The anion was exchanged by addition of a concentrated solution of 7.8 g $NaSbF_6$ (Fluka). The salt could be isolated by addition of the double volume of ice water. This liquid salt was dissolved in

Table 1
Spectroscopic data of the salts used (DS_1 as SbF_6^-, DS_2 and DS_3 as PF_6^-)

Salt	UV–VIS		IR $\tilde{\nu}$ (cm^{-1})	^1H NMR in $CDCl_3$, δ (ppm)
	λ_{max} (nm)	ε ($l\,mol^{-1}\,cm^{-1}$)		
DS_1	315	24460	2245	7.1470 (d, 2H, $J = 9.33$ Hz), 8.3424 (d, 2H, $J = 9.48$ Hz)
DS_2	277, 348	14080, 4860	2264	7.0642 (s, 1H), 7.1295 (d, 1H, $J = 8.76$ Hz), 8.2769 (d, 1H, $J = 8.61$ Hz)
DS_3	287, 377	11850, 4050	2237	6.9418 (d, 2H, $J = 8.79$ Hz)[a], 8.0844 (t, 3H, $J = 8.77$ Hz)[a]

[a] Values in acetonitrile-d_3.

methylene chloride. Additionally, the dried CH_2Cl_2 solution was purified by passing through a short cellulose column. The liquid salt (obtained by careful remove of solvent) was dried over P_4O_{10} under reduced pressure; yield = 80%.

Spectroscopic data of the salts are summarized in Table 1.

2,5-Di-(butyloxy)-4-morpholinobenzenediazonium hexafluorophosphate was obtained from Synthec Wolfen. The α,ω-epoxy terminated disiloxane EP (see Scheme 1) was an experimental product of Wacker-Chemie Burghausen. The epoxy content of the silicone derivative is larger than 97% (NMR-spectroscopy). The synthesis of EP has been described elsewhere [12]. The vinyl ether derivative DVE and DVE-3 were commercial products (Aldrich).

2.2. Measurements

Absorption spectra were recorded on a UV–VIS–NIR spectrophotometer UV-3101 PC (Shimadzu). Thermolysis of the diazonium salts was investigated in different solvents in black glass vessels. The temperature was adjusted to 40 ± 1°C. Decomposition of the onium salt was determined by UV-spectroscopy. The starting concentrations of the diazonium salt solutions were adjusted for an optical density of approximately 2.0 in the absorption maxima. Fast thermal reactions, i.e. reaction between diazonium salt and monomer, were directly carried out in the UV-spectrometer in a thermostated cell. The decrease of optical density at a selected wavelength (usually the absorption maximum) was used for the evaluation by a biexponential model of a first-order law; see Eq. (1). The rate constant was determined by nonlinear regression

$$E = E_{DS}\,e^{-kt} + E_{Prod}(1 - e^{-kt}) \quad (1)$$

where E is the sum of the optical density of the diazonium salt (E_{DS}) and of the product (E_{Prod}), k the rate constant and t the time.

The molecular parameters were calculated with HyperChem (Hypercube) software. The molecular geometry was optimized by means of the Polak–Ribiere method (gradient $= 0.0005\,kcal\,mol^{-1}\,Å^{-1}$). The electronic structure was optimized using the semi-empirical PM3-method (charge: +1 and the spin-multiplicity: 1). The SCF-convergence was limited to 1×10^{-5} and the spin pairing was treated with the RHF-method, which accepts the same energy for paired electrons with different spin.

The half-wave potentials were measured with a AUTOLAB PG STAT 20 (Eco Chemie) potentiostat with a voltage feed of $100\,mV\,s^{-1}$. The cell contained a stirrer, a device for working under inert gas, working-, counter-, and reference-electrodes of platinum (working-electrode: platinum-pin; length = 5 mm; diameter = 0.5 mm, counter-electrode: platinum-pin; length = 5 mm; diameter = 0.5 mm; reference-electrode: platinum-sheet; area = $112\,mm^2$). Dry acetonitrile (Aldrich) solutions of tetra-*n*-butylammonium hexafluorophosphate ($0.1\,mol\,l^{-1}$) and tetra-*n*-butyl-ammonium hexafluoroantimonate ($0.1\,mol\,l^{-1}$) were used as electrolyte, respectively. The solution was bubbled with nitrogen. Ferrocene ($U = 0.48\,V^{SCE}$) served as a reference compound for the calibration with the standard calomel electrode (SCE).

The construction of the isoperibolic calorimeter has been schematically described previously [13]. Hardware and software were modified (Rittmeier, Computeranwendungen, Merseburg). The filter 1602 (Jenaer Glas-Werke Schott und Gen.) was used to select the wave-length region from 270 to 380 nm of the emitted light of a 200 W high-pressure mercury arc lamp (HBO 200, Narva). The most intense lines at 365 and 313 nm show the ratio 1:0.4. For measurements, 20 μl of the formulation were put on a Ni-plate that was connected with the probe thermistor (∅ = 1 cm). An equal amount of initiator, dissolved in diethylene glycol dimethyl ether (Fluka) was applied as reference. The thickness of the samples was about 270 μm.

The standard heat of polymerization of epoxides ($94.5\,kJ\,mol^{-1}$ [14]) was used in order to calculate the conversion degree. Using reaction enthalpy for the silicone epoxide EP ($\Delta H = 55.3\,kJ\,mol^{-1}$ [9]) resulted in conversions larger than 100%. Presumably, the value of $55.3\,kJ\,mol^{-1}$ was determined as result of an impeded crosslinking, see also [9].

A mixture of 1,2-dichloroethane/methylene chloride (1:3) at 77 K was used as the matrix for the EPR-investigations. The sample tube (quartz) was irradiated in a Dewar-cooler (quartz) in the focus of a high-pressure mercury arc lamp (HBO 200, Narva) through a combination of heat protection plate and the filter combination 1602 + UV KIF 313 (Jenaer Glaswerke Schott und Gen.). Measurements were made in the resonator H_{102} (ERS 220 ZWG Berlin-Adlershof, X-band, 100 kHz modulation, modulation amplitude = 3.5 Oe). Determinations of the signal position in the magnetic field was measured with the proton resonance magnetometer (MJ 110-R, Radiopan) and the frequency with a frequence divider and an electronic counter (5260 A, 5261 A and Hewlett-Packard, respectively).

A software for powders was used [15] for the simulation of the EPR-spectra.

Nuclear magnetic resonance spectra were obtained on a GEMINI 300 (300 MHz) from Varian. The solvents chloroform-d and acetonitrile-d_3 were received from Aldrich.

3. Results and discussion

3.1. Photocrosslinking

3.1.1. General crosslinking kinetics

Eq. (2) can describe the rate of the photocrosslinking process (R_P) in bulk under stationary irradiation conditions:

$$R_P = -\frac{d[M]}{dt} = -\frac{dx}{dt}[M]_0 = k(x)[M]^\alpha I_0^\beta \quad (2)$$

where [M] is the molar concentration of polymerizable functional groups, t the time, $k(x)$ a conversion (x) dependent quantity reflecting the effect of the actual surroundings on the reaction partners, I_0 the intensity of the incident light, α and β the exponents.

That general expression can reliably describe bulk polymerization in detail because rate constants for propagation and termination change as a function of conversion [16,17]. The exponent β gives information about termination mechanisms. The following relationships can be outlined for β [16,17]:

- $\beta = 1$, first-order termination;
- $0.5 < \beta < 1$, mixed first- and second-order termination;
- $\beta = 0.5$, second-order termination.

The kinetics of the photo-induced cationic crosslinking differs with respect to the thermally-induced crosslinking only in the initiation step. According to Eq. (2), the dependence of R_P on I_0 can be deduced only from the initiation rate R_i in Eq. (3) (see also [16]). Under this assumption Eq. (4) is derived:

$$R_i = \eta \Phi_{H^+} \eta_{abs} I_0 \quad (3)$$

$$R_P = k'(x)[M]^\alpha (\eta \Phi_{H^+} \eta_{abs} I_0)^\beta \quad (4)$$

where R_i is the initiation rate, η the addition efficiency of the initially-formed proton to the monomer, η_{abs} the fraction of the absorbed light, Φ_{H^+} the quantum yield of proton formation, $k'(x)$ a conversion dependent quantity.

The inhibition time t_i reflects the generation of the initiating species in the system used [16,18] corresponding to Eq. (5)

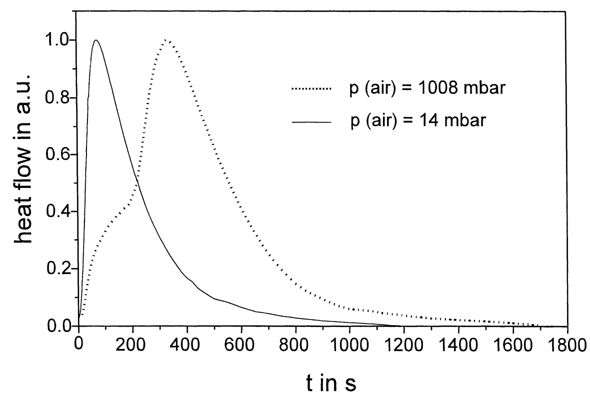

Fig. 1. Measured heat flow in the crosslinking of the system EP/DS_1 under air and under reduced pressure ($[DS_1] = 2 \times 10^{-2}$ mol l^{-1}; DS_1 as SbF_6^-, $I_0 = 2$ mW cm^{-2}).

$$t_i = \frac{[Q]}{R_i} = \frac{[Q]}{\eta \Phi_{H^+} \eta_{abs} I_0} \quad (5)$$

where [Q] is the inhibitor concentration.

3.1.2. Photocrosslinking using diazonium salts

Fig. 1 shows typical profiles of the measured heat of polymerization as a function of time for the system EP/DS_1 under air and inert conditions during irradiation. The rate of polymerization (R_P) and the conversion can be obtained at selected reaction times from the heat flow value if the standard reaction heat is known for the system used, see Eq. (6). Nevertheless, the time constants of our photocalorimeter requires deconvolution of the measured curve [13]; see also [19].

$$R_P = -\frac{d[M]}{dt} = -\frac{dx}{dt}[M]_0 = -\frac{dH}{dt}\frac{[M]_0}{\Delta_R H^0} \quad (6)$$

where dH/dt is the heat flow of the reaction, $\Delta_R H^0$ the standard reaction enthalpy of the crosslinking.

Fig. 2 shows the behavior of R_P corresponding to Eq. (2). For kinetic discussion, the maximum value of R_P was used. The plot R_P versus I_0 shows linear behavior, which stands in agreement with ideal cationic polymerizations because

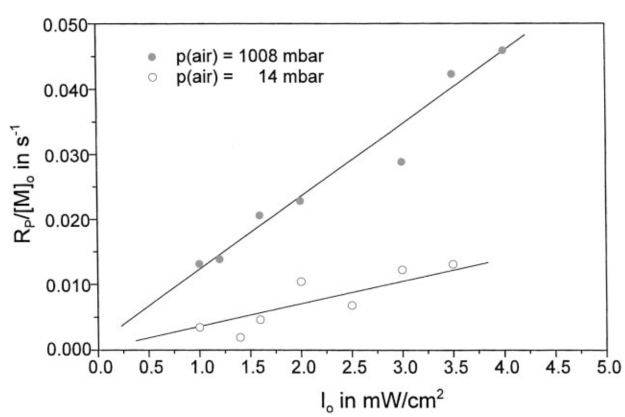

Fig. 2. Influence of light intensity I_0 on the polymerization rate under air and under reduced pressure; experimental conditions see Fig. 1.

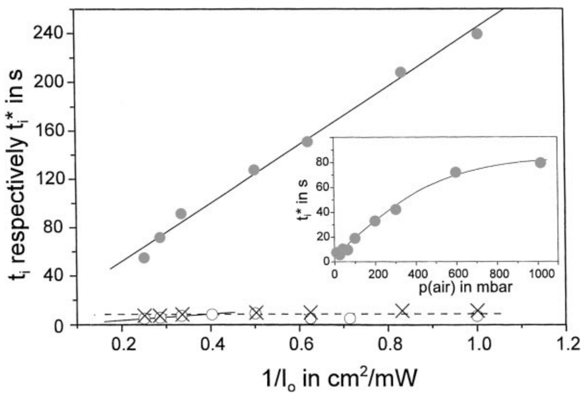

Fig. 3. Inhibition times t_i and t_i^* (see text) as function of the light intensity I_0 ((○) t_i under 14 mbar, (×) t_i under normal pressure, (●) t_i^* under normal pressure). Inset: t_i^* value (●) as a function of the air pressure, for experimental conditions see Fig. 1.

termination reaction follows a first-order law ($\beta \approx 1$). Moreover, crosslinking starts after a short inhibition phase caused by the presence of a small amount of impurities. Under ideal conditions, the value of the induction period depends on the inhibitor concentration as well as on the incident light intensity, see Eq. (5). Fig. 3 shows the relationship between t_i and $1/I_0$. The t_i value does ranges in the detection limit. Therefore, a plot of t_i against $1/I_0$ is difficult for evaluation.

Cationic polymerization should not depend on atmospheric conditions. Surprisingly, the heat flow measured for the EP/DS system differs under air and inert conditions; see Fig. 1. A strong additional shoulder can be observed under air. The mathematical treatment of the heat flow shows that two local polymerization maxima of the rate exist in the rate/time profile, see Fig. 4. Moreover, the second process is synergetic with the crosslinking reaction and results in an increased rate and higher conversion. Interestingly, the inhibition time t_i shows the same behavior either under air or oxygen free conditions, see Fig. 3.

The inhibition time can be obtained from the intersection of the slope of the conversion/time plot (R_{max}) with the

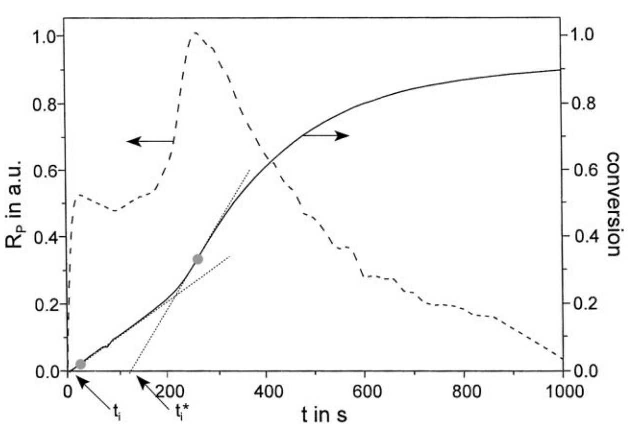

Fig. 4. Conversion and reaction rate R_P as functions of the irradiation time t; air, further experimental conditions see Fig. 1.

x-axis. The mathematical separation leads to a second (formal) t_i^* value for the second local maximum of R_P, which is linear versus $1/I_0$, see Fig. 3.

The inhibition time is related to the efficiency of cation generation; see Eq. (5). Interestingly, t_i^* shows a strong dependence on the presence of oxygen; see the inset in Fig. 3. In other words, oxygen inhibits the formation of the cationic initiating species. On the other hand, the reaction rate increases under oxygen. Nevertheless, in comparison to crosslinking under inert conditions, the time to reach the maximum value of R_P is delayed under air.

Crosslinking of the vinyl ether derivatives was similar results to epoxy crosslinking. However, the thermal instability of the formulations allows only single measurements. It prevents an extensive study of the crosslinking kinetics. The influence of oxygen on the crosslinking of vinyl derivatives is in the same direction.

3.1.3. Postpolymerization

The photo-induced crosslinking allows one to stop the initiation of the crosslinking reaction at a defined time (t_{ex}) by a simply switching off the light [6,7,17,18]. So the kinetics of the crosslinking is simplified to propagation and termination reactions. The conversion of the monomer in the dark period (x_D) after initiation corresponds to Eq. (7); see [17]:

$$-\ln(1 - x_D) = \frac{k_p}{k_t}[P^+]_0(1 - e^{-k_t t}) \qquad (7)$$

where x_D is the double bond conversion in the dark period, $[P^+]_0$ the polymer cation concentration at beginning of

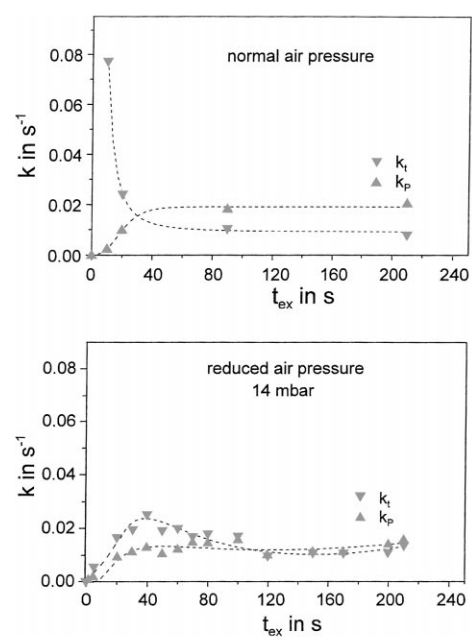

Fig. 5. Rate constants of propagation (k_p) and termination (k_t) as function of the irradiation time t_{ex} (system EP/DS$_1$; $[DS_1] = 2\times10^{-2}$ mol l^{-1}; DS$_1$ as SbF_6^-, $I_0 = 3$ mW cm^{-2}; top: under air; bottom: reduced pressure).

Association		*Ionization*		*Dissociation*
$(A\text{-}B)_n$ $\rightleftharpoons$	$A^{\delta+}\text{-}B^{\delta-}$ $\rightleftharpoons$	$A^{\oplus}\,B^{\ominus}$ $\rightleftharpoons$	$A^{\oplus}$/solvent/$B^{\ominus}$ $\rightleftharpoons$	$A^{\oplus} + B^{\ominus}$
covalent bond	polarized covalent bond	contact ion pair	solvent separated ion pair	free ions

Scheme 2.

postpolymerization, k_p the polymerization rate constant, k_t the termination rate constant.

One can estimate the parameters of Eq. (7) by means of standard nonlinear regression. Postpolymerization experiments were made to study the effect of oxygen on the propagation and termination steps. The results of our study are summarized in Fig. 5.

As expected, k_p is nearly independent on the atmospheric conditions. The k_p value increases asymptotically with increasing irradiation time t_{ex}. At longer t_{ex} times, k_p approaches a constant value. Surprisingly, our results show a strong dependences of the termination step on the atmospheric condition. Under inert conditions, the k_t value possesses small numbers, increases, reaches a maximum and approaches a constant value at prolonged irradiation time. Such behavior suggests that only a small amount of inhibitor is present in the formulation. Moreover, the increasing k_t could be caused by immobilization of the reactive chain end.

However, a very effective inhibition was found under air. The k_t starts at a high level and decreases with increasing irradiation time t_{ex}. These facts show that oxygen influences the termination reaction. This effect is surprising since k_t is a function of a cationic process and should not show any interaction with oxygen. Obviously, the influence of oxygen on the system results in the generation of a cationic inhibitor. Oxygen loses its influence as a result of increasing viscosity.

3.1.4. Effect of anions

Free cations on the polymer chain facilitate attack on the monomer. The active center of the growing chain is influenced by the electrostatic forces between the cation and the anions. Association, ionization or dissociation equilibria of the active bond A–B [20] described the system; see Scheme 2. The strength of the equilibrium depends on both nucleophilicity and size of the anion. Larger anions result in a shift of the equilibrium towards free ions. Thus, only the SbF_6^- salt [1] of DS_1 possesses the capability to initiate the photopolymerization of the epoxide derivative EP.

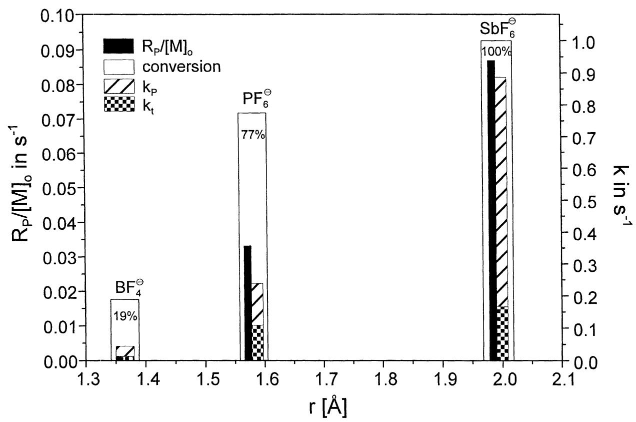

Fig. 6. Influence of anions on the polymerization parameters (system: DVE-3/DS_1; $[DS_1] = 1.5 \times 10^{-2}\,mol\,l^{-1}$; $I_0 = 2\,mW\,cm^{-2}$; $t_{ex} = 40\,s$; air).

The influence of the anion size on the polymerization can be demonstrated by the use of the vinyl ether derivative DVE-3. The dependence of polymerization on the BF_4^-, PF_6^- and SbF_6^- anions are summarized in Fig. 6. As can be seen, k_p increases with the increasing anionic radius. The influence of the anion is stronger on the propagation step than on the termination step. Therefore, the highest reaction rate occurs using the SbF_6^- anion. The PF_6^- yields to a solid, colorless vinyl ether polymer with a hard, non-tacky surface. Because the polymerization is highly exothermic, the SbF_6^- salt causes dark colored polymers. In contrast, BF_4^- ions promote an inefficient crosslinking and results in a polymer with a sticky surface. The $B(C_6F_5)_4^-$ salt of DS_1 initiates immediately upon mixing resulting in a spontaneous rapid thermally-induced polymerization.

3.1.5. EPR-study

Photolysis of the diazonium salts is independent of oxygen in several organic solvents (acetonitrile, 1,2-dichloro-ethane, dimethoxyethane) [21]. These results and flash photolysis experiments [21,22] show that the salts decompose by photo-

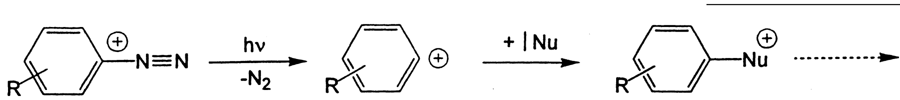

(8a)

heterolysis (Eq. (8a)) in these solvents. A mass spectroscopy study [21,22] of the photoproducts support that result. Nevertheless, fluorinated products, which can be formed in a

[1] The BF_4^--salt of DS_1 is insoluble in EP, the $B(C_6F_5)_4^-$-salt of DS_1 starts a thermally-induced polymerization (shelf-stability of the formulation = 3 min).

photo-Schiemann [23,24] reaction (see Eq. (8b)), not have been observed.

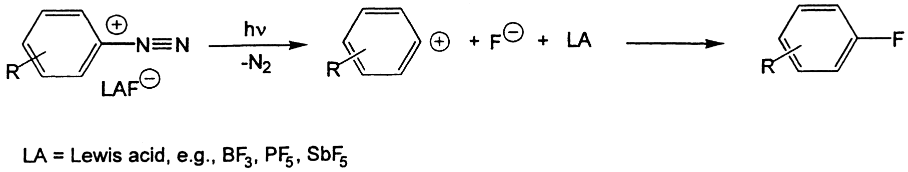

(8b)

The influence of oxygen on the cationic crosslinking shows that radical reactions dominant during the crosslinking process. Therefore, the photolysis of the diazonium salt/monomer (epoxide or vinyl ether) mixture was investigated by EPR in a glassy matrix (77 K; 1,2-dichloroethane/methylene chloride mixture; volume:volume = 1:3).

The EPR-experiments prove that radicals were formed during the photolysis; see Fig. 7. The photolysis of the diazonium salt in the different monomer systems results in a similarly shaped EPR-signal. Moreover, the independence of the monomer's signal shape shows that the observed radical is a photoproduct of the diazonium salt. Possible products are: (1) a diazenyl radical formed by electron transfer and (2) an aryl radical formed as fragmentation product of the diazenyl radical; see Scheme 3.

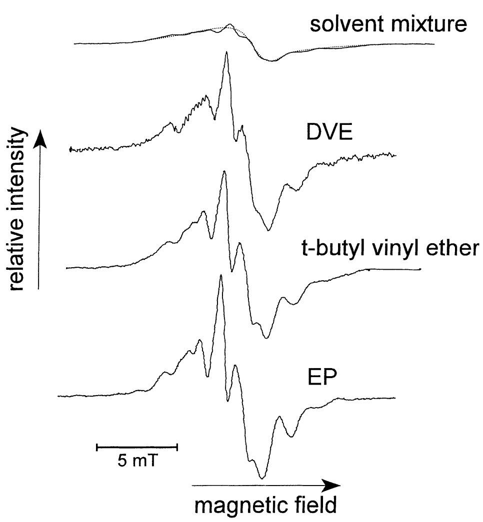

Fig. 7. EPR-signals obtained under irradiation of the diazonium salt DS_1 without (top) and with monomer (bottom) in a solution of 1,2-dichloroethane/methylene-chloride (1:3) at 77 K (DS_1 as hexafluoro-phosphate, $\lambda = 313$ nm, $[DS_1]$: saturated, [monomer] ≈ 0.5 mol l^{-1}).

The hyperfine splitting predicted for these two radicals are sketched in Fig. 8. A group of nine single peaks are predictul to appear in both the diazenyl radical and in the aryl radical, respectively. However, both signals differ in the relative signal intensities. Comparing the experimental and the calculated spectra suggests an aryl radical is present rather than a diazenyl radical given equal intensities of the hyperfine lines, see also [25]. Nevertheless, the observed EPR line shape differs from the calculated. Presumably, the effect was caused by a superposition with a signal of other paramagnetic species.

This hypothesis is supported by EPR-signals obtained by photolysis of the diazonium salt in the glassy matrix without the monomer; see Fig. 7. A broad signal with small spikes was detected, which can be interpreted as superposition of a large broad unstructured paramagnetic signal with a small part one of an aryl radical signal; see upper traces in Fig. 7. Fig. 8 shows that the superposition of the broad unstructured paramagnetic signal with a higher concentration of the aryl radical agrees very well with the experimental signal obtained during the photolysis of the monomer/diazonium salt matrix. This may be compare with Fig. 7 (spectra with DVE, *tert*-butyl vinyl ether, and EP, respectively). Thus, these EPR-measurements confirmed the generation of aryl radicals by photolysis of arene diazonium salts in the presence of epoxide and vinyl ether. The position of the signal corresponds to literature values with a typical *g*-factor of $\approx$2.003 [26,27]. The photolysis of the diazonium salt in the presence of vinyl ether derivatives or epoxides is accompanied by the oxidation of the monomer; see Scheme 3. Moreover, the photo-induced electron transfer starts the Meerwein-reduction of the diazonium salt.

Nevertheless, aryl radicals can be formed also from aryl cations in the triplet-state; see Eq. (9) [28]. Our EPR-experiments show no signal at half magnetic field intensity, which is typical for a triplet. The half-field signal corresponds to a $\Delta m = 2$ transition which can occur only in a system with two unpaired electrons. Triplet cations were detected in the case of 2,5-di-(hexyloxy)-4-morpholinobenzenediazonium

$$\mathrm{DS^{\oplus} + M \xrightarrow{h\nu} Ar\text{-}N{=}N\cdot + M^{\cdot\oplus}}$$
$$\mathrm{Ar\text{-}N{=}N\cdot \longrightarrow Ar\cdot + N_2}$$
$$\mathrm{Ar\cdot + R\text{-}O\text{-}CH_2\text{-}CH_2\text{-}R' \longrightarrow R\text{-}O\text{-}\dot{C}H\text{-}CH_2\text{-}R + Ar\text{-}H}$$
$$\mathrm{DS^{\oplus} + R\text{-}O\text{-}\dot{C}H\text{-}CH_2\text{-}R \xrightarrow[-N_2]{} R\text{-}O\text{-}\overset{\oplus}{C}H\text{-}CH_2\text{-}R + Ar\cdot}$$
$$\mathrm{R\text{-}O\text{-}\overset{\oplus}{C}H\text{-}CH_2\text{-}R \longrightarrow R\text{-}O\text{-}CH{=}CH\text{-}R + H^{\oplus}}$$

Scheme 3.

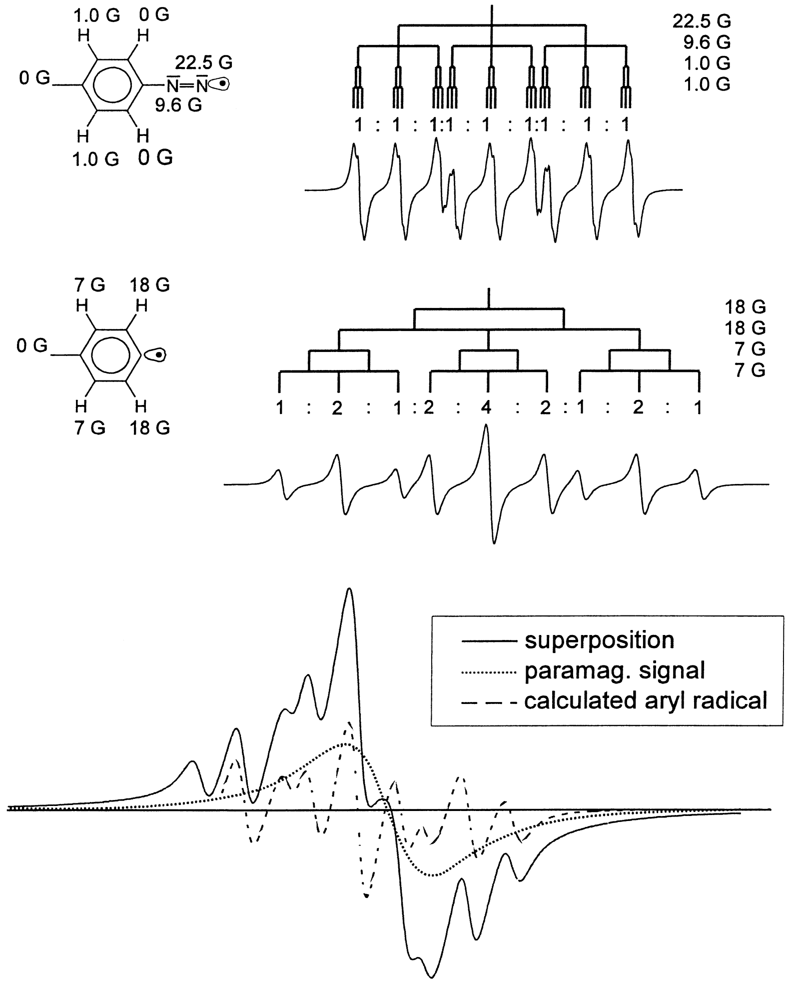

Fig. 8. Top: hyperfine structure of the expected EPR-signals of aryl and diazenyl radicals [25–27]; bottom: superposition of the aryl radical with one of the paramagnetic impurities.

hexafluorophosphate, see Fig. 9. Sign, contour and g-value are similar to the literature [29]. The signal at H_0 can be divided, according to Kemp [29], into the aryl radical.

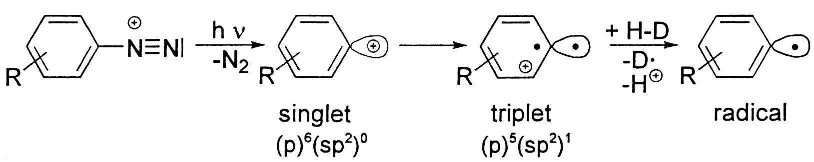

(9)

The absence of the triplet cation radical in the case of 4-hexyloxy-benzene diazonium hexafluorophosphate shows that the aryl radicals can be exclusively formed by an electron transfer; see also [29].

Nevertheless, EPR-measurements prove that a second radical source exists in an oxygen saturated vinyl ether solution under irradiation. Under these conditions, one can observe CT-complex formation between the vinyl derivative and oxygen, see Fig. 10. The reversibility of this effect excludes oxidation. The excitation of this complex results in a radical formation; see Fig. 10. Presumably, the mechanism of the radical formation is like the UV-initiated autooxidation of hydrocarbons [30].

3.1.6. Thermodynamic considerations

The EPR-study shows that the photocrosslinking starts with a photo-induced electron transfer from the monomer to the diazonium salt. Radical cations originating from the monomer are formed. These can initiate the cationic crosslinking of the monomer themselves or by their consecutive products. Moreover, the aryl radicals-induced a second thermal initiated cation formation, which is the Meerwein-reduction of the diazonium salt, see Scheme 3. The free radical reduction of onium salts is well known for

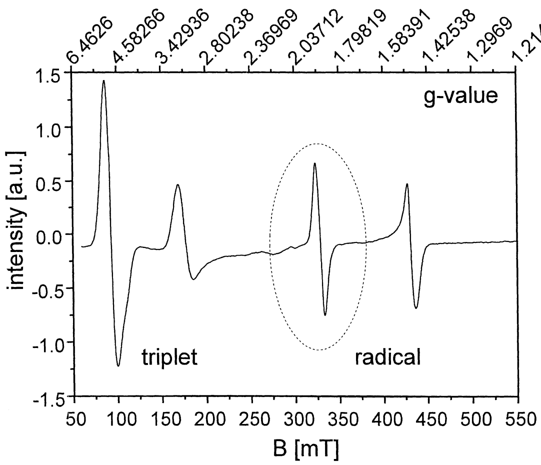

Fig. 9. Superposition of the EPR-signals of the triplet-cation and aryl radical obtained by irradiation of 2,5-di-(butyloxy)-4-morpholino-benzenediazonium hexafluorophosphate in a 1,2-dichloro-ethane/methylene chloride (1:3) solution at 77 K ([salt]: saturated).

diazonium [24,31,32], iodonium [31,33–36] and sulfonium salts [31,35,36].

These reactions are thermodynamically possible, if the conditions of Eq. (10) are fulfilled:

$$\Delta G = (E_{\mathrm{ox}}^{\mathrm{radical}} - E_{\mathrm{red}}) < 0 \tag{10}$$

where ΔG is the free energy of the electron transfer, $E_{\mathrm{ox}}^{\mathrm{radical}}$ the half-wave oxidation potential of the radical, E_{red} the half-wave reduction potential of the onium salt.

The energetics given in Fig. 11 show that the thermodynamic conditions of Eq. (10) become a reality for several radicals and onium salts. Thermodynamics also show that an electron transfer between the monomer and onium salt is forbidden in the ground state. The electron transfer is allowed only after excitation of the onium salt; see Eq. (11). Furthermore, thermodynamics show that oxy radicals, which were formed during radical scavenging by oxygen, cannot reduce onium salts in the dark. Nevertheless, the potential of the peroxy radicals lies in a critical range where an electron transfer to the diazonium salt is possible.

$$\Delta G = (E_{\mathrm{ox}} - E_{\mathrm{red}} - {}^{*}E) < 0 \tag{11}$$

where E_{ox} is the oxidation potential of the reaction partner (monomer, radical, etc.), ${}^{*}E$ the energy of the excited state of the onium salt.

The electron transfer mechanism explains the influence of oxygen on the cationic crosslinking kinetics. Formation of the initiating species occurs by a photo-induced electron transfer reaction. That reaction is independent on the oxygen concentration. Consequently, one observes the same inhibition time for crosslinking under air as well as under inert conditions. Oxygen prevents or retards the possibility of the Meerwein-reduction, which results in a reduced crosslinking rate in the start phase of the crosslinking; see the shoulder in Fig. 1.

Moreover, radical scavenging by oxygen (see Scheme 4) results in the formation of water and alcohols, which are well known as inhibitors of the cationic crosslinking [20]. These reactions caused differences in the termination of the cationic crosslinking in the presence of air and under inert conditions. Nevertheless, the role of water and alcohols depends on the concentration, monomer and initiator used. The role of small amounts of water or alcohol as co-initiator in cationic polymerization has been well described [20], if Lewis acids act as initiators.

The low reaction rate in the start phase is under air combined with a strong increase of the reaction rate after a

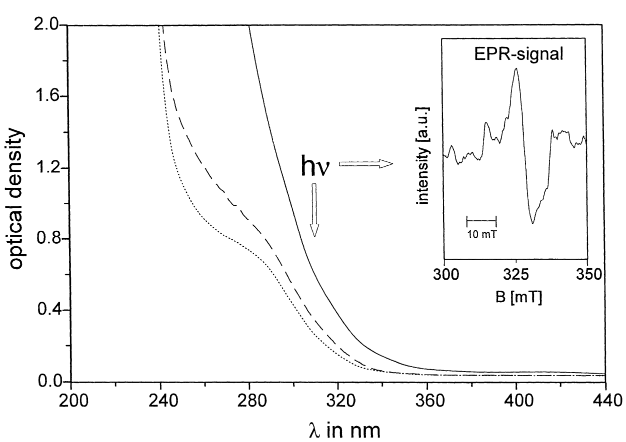

Fig. 10. UV spectra of DVE saturated with argon (. . .), air (– –) and oxygen (—); inset: EPR-sign during excitation of an oxygen saturated DVE/1,2-dichloroethane/methylene chloride mixture at 77 K (λ = 313 nm).

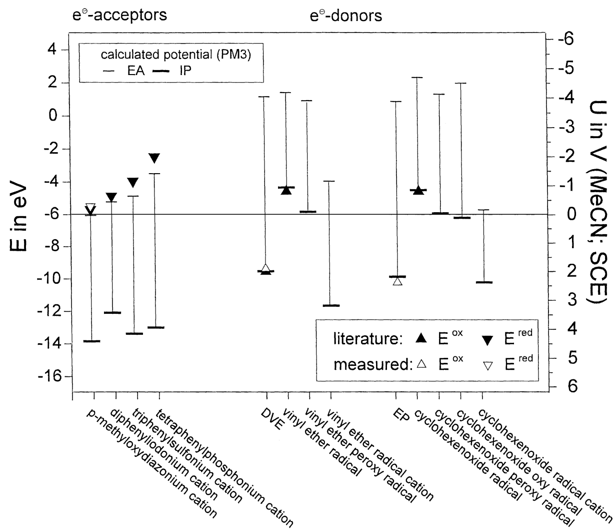

Fig. 11. Comparison of calculated ionization potentials (IP) and electron affinities (EA), oxidation and reduction potentials of several onium salts as e$^-$-acceptors and monomers and radicals as e$^-$-donors (literature values: $E_{\mathrm{red}} = -0.175$ V per diazonium [39]; -0.64 V per iodonium [41]; -1.1 V per sulfonium [41]; -2.0 V per phosphonium [42]; $E_{\mathrm{ox}} = 1.998$ V per vinyl ether [40]; -0.808 V per vinyl ether radical [35]; -0.808 V per cyclohexenoxide [35]).

$$\cdot\mathrm{R} + \mathrm{O_2} \longrightarrow \mathrm{R\text{-}O\text{-}O\cdot}$$
$$\mathrm{R\text{-}O\text{-}O\cdot} \xrightarrow{+\mathrm{M}} \mathrm{R\text{-}O\text{-}O\text{-}H} + \cdot\mathrm{M}$$
$$2\,\mathrm{R\text{-}O\text{-}O\cdot} \rightleftharpoons \mathrm{R\text{-}O\text{-}O\text{-}O\text{-}O\text{-}R} \longrightarrow 2\,\mathrm{R\text{-}O\cdot} + \mathrm{O_2}$$
$$\mathrm{R\text{-}O\text{-}O\text{-}H} \longrightarrow \mathrm{R\text{-}O\cdot} + \cdot\mathrm{O\text{-}H}$$
$$\mathrm{R\text{-}O\text{-}O\text{-}H} \xrightarrow{+\mathrm{M}} \mathrm{R\text{-}O\cdot} + \mathrm{H_2O} + \mathrm{M\cdot}$$
$$2\,\mathrm{R\text{-}O\text{-}O\text{-}H} \longrightarrow \mathrm{R\text{-}O\text{-}O\cdot} + \mathrm{R\text{-}O\cdot} + \mathrm{H_2O}$$
$$\mathrm{R\text{-}O\cdot} \xrightarrow{+\mathrm{M}} \mathrm{R\text{-}O\text{-}H} + \cdot\mathrm{M}$$
$$\mathrm{H\text{-}O\cdot} \xrightarrow{+\mathrm{M}} \mathrm{H_2O} + \cdot\mathrm{M}$$
$$2\,\mathrm{R\text{-}O\cdot} \rightleftharpoons \mathrm{R\text{-}O\text{-}O\text{-}R}$$

Where R· represents all radicals and as M reacts with the O-CH_2-CH_2-unit of the spacer

Scheme 4.

defined conversion; see Fig. 2. Presumably, increase of viscosity reduces the oxygen diffusion due to the crosslinking process. The secondary radical-induced cation formation gains more importance. Additional amounts of cations were generated and the reaction rate increases. Moreover, the higher reaction rate is related to a stronger heat flow, which accelerates the decomposition of the formed peroxides resulting in a branched radical reaction and finally in an explosion like cation formation. The reaction rate is faster under air than under inert condition. The stronger color of air-crosslinked products (air: brown, inert: pale yellow) is caused by the stronger heat formation under air.

The peroxide effect mentioned is not limited to diazonium salts. Jönsson [36] found a relation between the amount of peroxide in the monomer and the temperature of spontaneous polymerization in vinyl ether/sulfonium salts and vinyl ether/iodonium salts formulations, respectively.

The radical-induced formation of initiating species (protons, cations, cation radicals) is the general problem for the formulation stability. An exposure time of 1 s is sufficient to initiate the polymerization of the epoxide/diazonium salt formulation under inert condition. Reaction rate and conversion are not significant smaller than under continuous irradiation. This effect surprises even because the exposure time is shorter than the inhibition time ($t_i > 4$ s) under continuous irradiation. Nevertheless under air, when all radical reactions were quenched, polymerization starts only after an exposure time longer than the inhibition time.

These experiments show that using diazonium salts as photoinitiators traces of radicals can initiate the cationic polymerization. From the data of the reduction potential of several onium salts, one can deduce that only onium salts with $E_{red} < -1$ V prevent thermal radical-induced formation of initiating species.

3.2. Thermostability of the monomer/arene diazonium salt formulation

3.2.1. Mechanistic aspects

The arene diazonium salts used possess a high thermostability in non-polar solvents at 40°C ($t_{1/2} \gg 12$ days) [21,22]. In contrast, the monomer/arene diazonium salt formulations show unexpected insufficient shelf-stability at room temperature. The shelf-stability increases with decreasing nucleophilicity of the used anion. Additionally, the shelf-stability of the vinyl ether formulation is lower ($t < 5$ h; 10^{-3} mol l^{-1} DS_1 as SbF_6^-) than those of epoxy formulation ($t \approx 24$ h; 2×10^{-2} mol l^{-1} DS_1 as SbF_6^-). Moreover, this effect was also observed at total darkness as well as in the presence of oxygen. These condition should exclude the photo-induced radical processes. The extreme thermoinstability of the vinyl ether/diazonium salt formulations requires an extensive study of this effect. Therefore, measurements of thermal-stability of the formulations were carried out mostly with vinyl ether derivatives.

The high thermal stability of the used salt in 1,2-dichloroethane ($k\,(40°\mathrm{C}) = 7 \times 10^{-5} \pm 3 \times 10^{-5}\,\mathrm{h}^{-1}$) drops significant in presence of a small amount of vinyl ether derivative. The decomposition of diazonium salt becomes more than 400 times faster in a solution containing 0.2 mol l^{-1} DVE ($k\,(40°\mathrm{C}) = 0.030 \pm 6 \times 10^{-5}\,\mathrm{h}^{-1}$) than in pure 1,2-dichlorethane and it is 18 times faster than in pure DME. The rate constant of the decomposition correlates with the monomer concentration, see Fig. 12. The linearity at low DVE concentration indicates a pseudo-first-order rate law. The curvature at larger concentrations results in, presumably, changing of the viscosity at larger DVE concentration. The absence of EPR-signals show that the thermolysis of the diazonium salt occurs in a reaction route without any radical.

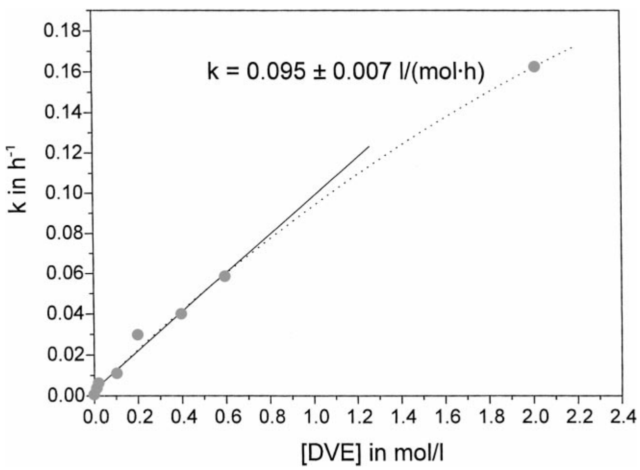

Fig. 12. Dependence of the first-order rate constant of the diazonium salt decay (k) at 40°C on the DVE concentration in 1,2-dichloroethane ($[DS_1] = 4 \times 10^{-5}$ mol l^{-1}; DS_1 as SbF_6^-).

This behavior corresponds to the findings of Zollinger [24,37], who described the kinetics of arylation of substituted arenes using benzene diazonium tetrafluoroborate depending on the concentration of the arenes. The reaction rates of the arylation are linear functions for concentration of the arene. The results of the arylation were consistent with either an $A_N D_N$ mechanism [24,37] (S_N2), as given in Eq. (12a), or a two-step $A_N + D_N$ mechanism [24,37] ($S_N Ar$).

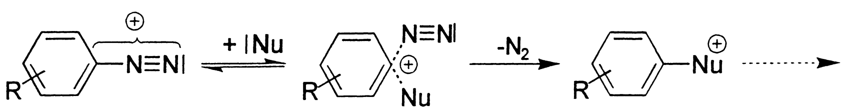

(12a)

Our findings of bimolecular dediazoniation and the results by Zollinger do not permit to distinguish between a concerted attack and the release of N_2, or the two-step mechanism. Both bimolecular mechanism described results in the dediazoniation without an intermediate aryl cation.

According this mechanism one can show that the attack of nucleophilic vinyl ether yields directly the initiating species of the cationic polymerization:

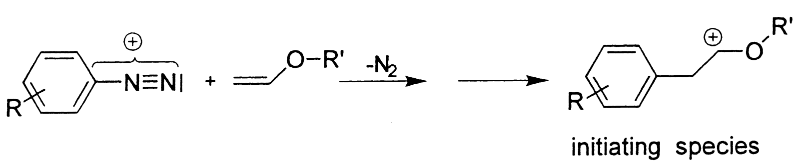

(12b)

The generation of the initiating species could explain the poor shelf-stability of the vinyl ether/diazonium salt formulation. Furthermore, the lower nucleophilicity of the epoxides explains the larger shelf-stability of the epoxide formulation. Additionally, the anion effect could be explained by the decreased electrophilic force of the diazonium salt. The size of the anions used influences the equilibrium between associates, ion pairs and free ions (shelf-stability of several DVE-3/DS_1-formulations: 60 (BF_4^-); 40 (PF_6^-) and 20 min (SbF_6^-); immediately after contact ($B(C_6F_5)_4^-$); $[DS_1] = 2 \times 10^{-2}$ mol l^{-1}; $\vartheta \approx 22$°C).

Moreover, the application of the above mechanism allows also to discuss the decomposition of diazonium salts in solution as solvolysis where the solvent reacts as nucleophile |Nu. Therefore, the diazonium salt decomposition depends on the nucleophilicity of the solvent.

Furthermore, the postulated mechanism should depend on steric effects. As a result, stability measurements were carry out with three electronic similar diazonium salts that have differences in their steric constitution; see Scheme 5. Interestingly, similar pseudo-first-order decomposition constants were determined in simple solvents like DME (DS_1: 1.7×10^{-3} h^{-1}; DS_2: 3.7×10^{-3} h^{-1}; DS_3: 2.9×10^{-3} h^{-1}; all salts as PF_6^-, $\vartheta = 40$°C). Significant differences were observed only in the case of vinyl ether formulation of the three salts mentioned. The two methoxy groups in the 2,6-position can sufficient stabilize the formulation. The observed stability shows that the mechanism of solvolysis and reaction with vinyl ethers is different. Presumably, either a π- or CT-complex between salt and olefinic system is involved as an intermediate in the above mechanism. A pale yellow shade of the thermoinstable DS_1 and DS_2 formulations support this assumption. The fact that the salt DS_3, which shows a similar thermal stability and similar quantum yield of the dediazoniation ($\Phi(DS_1) = 0.48, \Phi(DS_2) = 0.31, \Phi(DS_3) = 0.27$, all salts as PF_6^-, solvent: DME, $\lambda = 313$ nm, air) [21], is not able to photocrosslink the vinyl ether supports the protection of the diazonium salt with voluminous substituents.

3.2.2. NMR-study

Fig. 13 shows the NMR-spectra of a chloroform-d solution containing the salt DS_1 and *tert*-butyl vinyl ether.[2] After 2 h mixing the compounds, all signals of the vinyl ether disappear. The formation of new unstructured signals in the area of aliphatic resonance (1–2 ppm) and a broad signal at 3.47 ppm can be related to a polymer that is formed. The conversion of the diazonium salt and the decay of the vinyl ether were determined with the standardization of the signal integrals (internal standard: unchanged methylene groups at $\delta = 4.03$ ppm). The conversion time profile is given in

[2] *tert*-Butyl vinyl ether was used to reduced the quantity of signals.

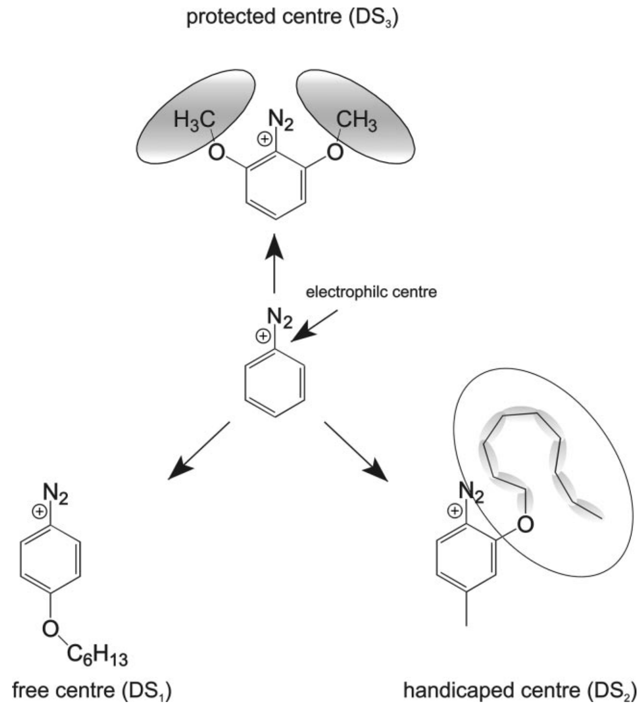

Scheme 5.

Fig. 14. Product formation and decay of the monomer possess similar rates. Interestingly, a significant decomposition of the diazonium salt was not detectable in that time. The non-polar solvent permits the cationic crosslinking of the vinyl ethers before a detectable amount of decomposition products of the diazonium salt was formed.

Fig. 15 summarizes the results of the NMR-study in an acetonitrile-d_3 solution. Thermolysis over 24 h yields in an unexpected large number of signals. Nevertheless, the basicity of acetonitrile prevents the polymerization of the vinyl derivative and allows to study product formation and decomposition of the diazonium salt. The time dependence of the signal integrals certifies a simultaneous loss of double bonds and decomposition of diazonium salt ($k = 0.13 \pm 0.02\,h^{-1}$).

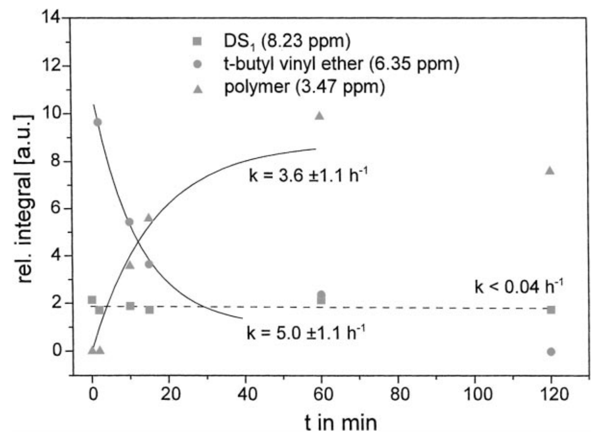

Fig. 14. Time profile of the NMR-signal integrals of DS_1, *tert*-butyl vinyl ether, and the formed polymer (all integrals were related to O–CH_2-signal of DS_1).

Moreover, an increment system [38] allows the classification of the signals by reference products expected for a non-adical pathway. Possible compounds are: (a) addition products of diazonium salts with release of nitrogen and (b) coupling products of the diazonium salts. One can deduce from this consideration method that the signal in group 1 corresponds to an azo-compound formed by a coupling reaction of the diazonium salt with the vinyl ether. Group 2 is equivalent to the tautomeric phenyl hydrazone. Group 3 was classified as an 4-alkylated arylether, which can be discussed as the product formed according Eq. (12b). Presumably, the poor band separation is caused form the interference of oligomer products. The classification of the doublet at 8.03 ppm has not been clear yet. Only strong electron withdrawing substitutes (nitro, carboxyl or positive charged groups) results in the chemical shift observed.

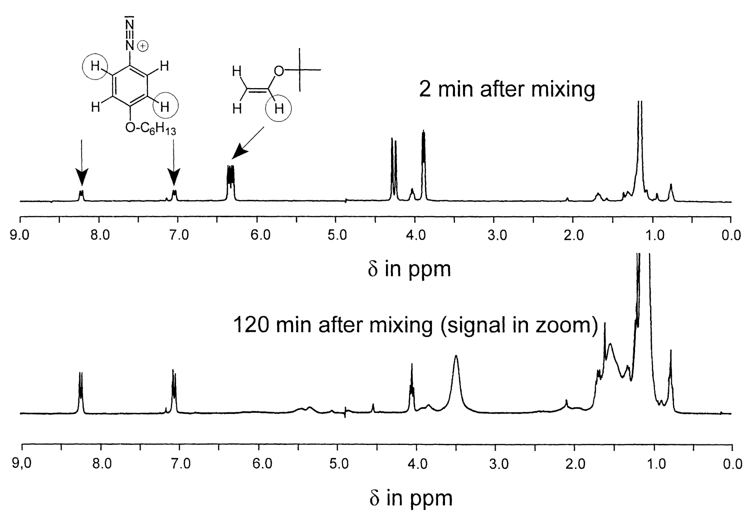

Fig. 13. ^{1}H NMR-spectra in the reaction of DS_1 with *tert*-butyl vinyl ether in chloroform-d at room temperature 2 and 120 min after mixing ([DS_1]: saturated; DS_1 as SbF_6^-; [vinyl ether]/[DS_1] ≈ 10).

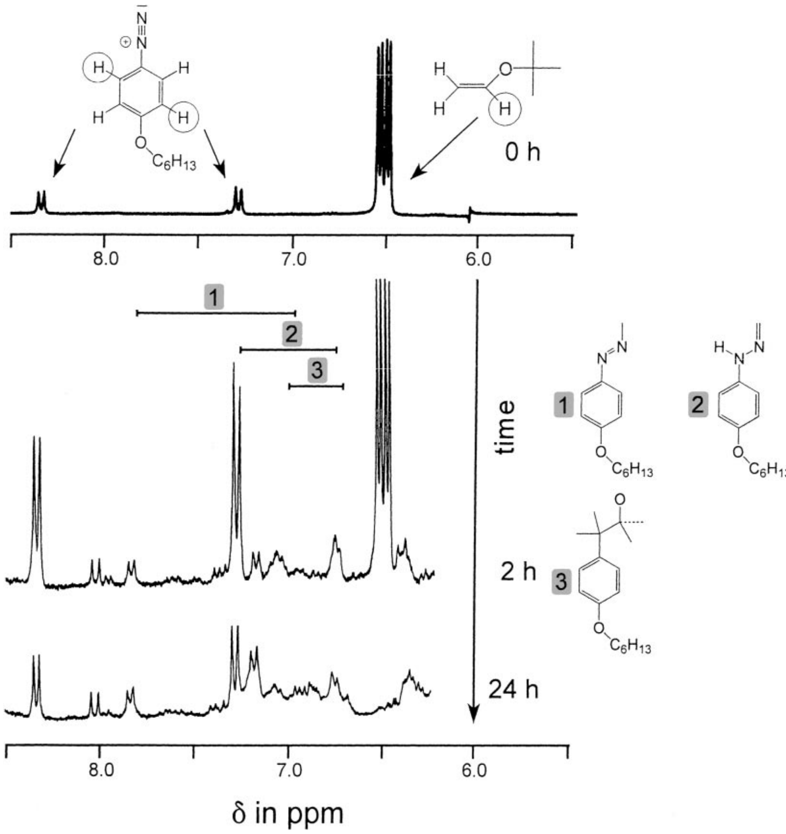

Fig. 15. ^{1}H NMR-spectra in the reaction of DS_1 with *tert*-butyl vinyl ether in acetonitrile-d_3 at room temperature immediately, 2 and 24 h after mixing ($[DS_1]$: saturated; DS_1 as SbF_6^-; [vinyl ether]/$[DS_1] \approx 10$).

The NMR-study supports the ionic reaction path of the thermolysis. Both the azo compound and the 4-alkylated arylether are consecutive products of a competitive reaction, see Eq. (12c).

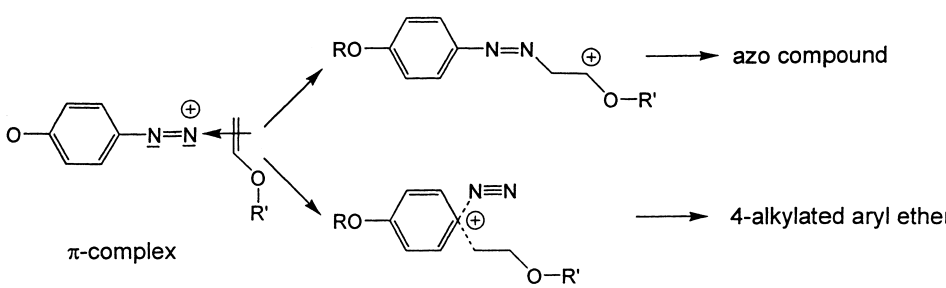

(12c)

4. Conclusions

4-Hexyloxysubstituted diazonium salts with complex anions like BF_4^-, PF_6^-, SbF_6^- and $B(C_6F_5)_4^-$ are compounds having a sufficient thermostability in several solvents. They strongly depend on the solvent used (dioxane: 12 days; 1,2-dichloroethane: 410 days). Moreover, the UV-absorption of these salts ($\lambda_{max} \approx 315$ nm; $\varepsilon \approx 27{,}000\,\mathrm{l\,mol^{-1}\,cm^{-1}}$) overlaps sufficient with the emission line of excimer lamps ($\lambda = 308$ nm). Additionally, no absorption of diffuse daylight and a high photosensibility ($\Phi \approx 0.4$) characterize these onium salts as compounds that should gain the attention for several applications.

The used salts initiate efficiently the photocrosslinking of vinyl ethers and epoxides. Cationic polymerization should occur independently on atmospheric conditions. Surprisingly, the measured reaction rate differs under air and inert conditions. A second maximum of the reaction rate can be observed under air. The reaction rate is faster under air than under inert conditions. Moreover, termination behavior of the cationic crosslinking depends on the atmospheric conditions.

The oxygen influence on the cationic crosslinking shows that radical reactions possess a key function in the crosslinking process. EPR-experiments proved that aryl radicals were formed by a photo-induced electron transfer between the monomer used and the diazonium salt. These experiment show that the mechanism of the cation formation strongly differs in an inert solution (photo-induced heterolysis) and in a reactive system (photo-induced electron transfer). Moreover, α-ether radicals as consecutive products of the aryl radicals can induce effectively the Meerwein-reduction of the diazonium salts. Oxygen inhibits the chain growth process. Furthermore, some reaction steps produce water and alcohol, which retard the cationic crosslinking. On the other hand, the decomposition of thermoinstable peroxides results in a branched radical reaction. Finally, the reaction rate becomes faster under air than under inert conditions.

The high thermostability of the SbF_6^--salt in 1,2-dichloroethane ($k\,(40^\circ C) = 7\times10^{-5}\pm3\times10^{-5}\,h^{-1}$) decreases by addition of a small amount of monomer. The decomposition of the diazonium salt increases in a solution that contains $0.2\,mol\,l^{-1}$ divinyl ether 400 times faster ($k\,(40^\circ C) = 0.030\pm6\times10^{-5}\,h^{-1}$) than in pure 1,2-dichloroethane and it is even 18 times faster than in pure dimethoxyethane. Absence of EPR-signals shows that thermolysis of the diazonium salt occurs according to non-radical way.

This behavior corresponds to the findings of Zollinger, which had discussed a bimolecular dediazoniation. Because vinyl ether derivatives act as nucleophilic compounds, the initiating cation of the cationic polymerization is directly produced without an intermediate aryl cation. Catalytic amounts of that intermediate catalyze the monomer decay. Therefore, dediazoniation products cannot be observed in non-polar solvents. Moreover, in polar medium, which inhibits the polymerization, one can observe a simultaneous decomposition of both the monomer and the diazonium salt. Dediazoniation products are detectable.

Our results show the poor thermal stability of the diazonium salts. These are: (a) peroxy content of the monomer and and (b) nucleophilicity of the monomer. Both effects demand a thermal formation of cations, which initiate the crosslinking reaction. The monomer and its byproducts are even the reason of the poor thermal stability of the diazonium salts and not as the assumed thermal instability of the salt used. Traces of radicals can initiate the cationic polymerization. Moreover, one can deduce that only onium salts with $E_{red} < -1\,V$ prevent the thermal radical-induced formation of an initiating species from the level of the reduction potential of several onium salts.

Acknowledgements

The authors are grateful to Wacker-Chemie GmbH for financial and material support and thank Wacker-Chemie GmbH for the permission to present these new findings.

References

[1] F. Lohse, H. Zweifel, Adv. Polym. Sci. 78 (1987) 61.
[2] H. Baumann, H.-J. Timpe, J. Prakt. Chem. 336 (1994) 377.
[3] U. Müller, Trends Photochem. Photobiol. 5 (1999) 117.
[4] J.V. Crivello, J.L. Lee, J. Polym. Sci., Polym. Chem. Ed. 27 (1989) 3951.
[5] J.V. Crivello, Adv. Polym. Sci. 62 (1984) 1.
[6] U. Müller, A. Kunze, Ch. Decker, Ch. Herzig, J. Weis, J. Macromol. Sci. Pure Appl. Chem. A 34 (1997) 1515.
[7] U. Müller, A. Kunze, Ch. Decker, Ch. Herzig, J. Weis, J. Macromol. Sci. Pure Appl. Chem. A 35 (1998) 203.
[8] J.V. Crivello, J.H. Lam, Macromolecules 10 (1977) 1307.
[9] R.P. Eckberg, in: J.P. Fouassier, J.F. Rabek (Eds.), Radiation Curing in Polymer Science and Technology, Vol. IV, Elsevier, London, 1993, p. 19.
[10] J.V. Crivello, K.D. Jo, J. Polym. Sci., Polm. Chem. Ed. 31 (1993) 2143.
[11] J.V. Crivello, R. Narayan, Macromolecules 29 (1996) 439.
[12] J.V. Crivello, J.L. Lee, J. Polym. Sci., Polym. Chem. Ed. 28 (1990) 479.
[13] H.-J. Timpe, B. Strehmel, F.-H. Roch, K. Fritzsche, Acta Polym. 38 (1987) 238.
[14] J. Brandrup, E.H. Immergut, Polymer Handbook, Wiley, New York, 1989.
[15] L.K. White, R.L. Belford, J. Am. Chem. Soc. 98 (1976) 4428.
[16] U. Müller, S. Jockusch, H.-J. Timpe, J. Polym. Sci., Polym. Chem. 30 (1992) 2755.
[17] H.-J. Timpe, B. Strehmel, Makromol. Chem. 192 (1991) 779.
[18] U. Müller, J. Macromol. Sci. Pure Appl. Chem. A 31 (1994) 1905.
[19] J.F. Rabek, in: J.P. Fouassier, J.F. Rabek (Eds.), Radiation Curing in Polymer Science and Technology, Vol. I, Elsevier, London, 1993, p. 329.
[20] J. Ulbricht, Grundlagen der Synthese von Polymeren, Vol. 2, Hüthig & Wepf Verlag Basel, Heidel-berg, New York, 1992.
[21] A. Utterodt, Thesis, Martin-Luther-Universität, Halle-Wittenberg, 1999.
[22] G. Israel, U. Müller, A. Utterodt, in preparation.
[23] H.G.O. Becker, G. Israel, J. Prakt. Chem. 256 (1979) 436.
[24] H. Zollinger, Diazo Chemistry I, VCH Verlagsgesellschaft mbH Weinheim, 1994.
[25] T. Suehiro, T. Tashido, R. Nakausa, Chem. Lett. 1980 1339.
[26] Landolt-Börnsteinin, in: A. Berndt, H. Fischer, H. Paul (Eds.), Zahlenwerte und Funktionen, NS II/9b, Springer, Berlin, Heidelberg, New York, 1977, p. 310.
[27] Landolt-Börnstein, in: H. Fischer (Ed.), Zahlenwerte und Funktionen, NS II/1, Springer, Berlin, Heidelberg, New York, 1965, p. 21.
[28] S.M. Gasper, C. Devadoss, G.B. Schuster, J. Am. Chem. Soc. 117 (1995) 5206.
[29] H.B. Ambroz, T.J. Kemp, J. Chem. Soc., Perkin Trans II 1979, 1420.
[30] R.D. Scurlock, P.R. Ogilby, J. Phys. Chem. 93 (1989) 5493.
[31] A. Ledwith, Polymer 19 (1978) 1217.
[32] H. Baumann, U. Müller, D. Pfeifer, H.-J. Timpe, J. Prakt. Chem. 324 (1982) 217.
[33] H.-J. Timpe, V. Schikowsky, J. Prakt. Chem. 331 (1989) 447.
[34] Y. Bi, D.C. Neckers, Macromolecules 27 (1994) 3683.
[35] P.-E. Sundell, S. Jönsson, A. Hult, J. Polym. Sci. Polym. Chem. 29 (1991) 1525.
[36] P.-E. Sundell, S. Jönsson, A. Hult, J. Polym. Sci. Polym. Chem. 29 (1991) 1535.
[37] P. Burri, H. Zollinger, Helv. Chim. Acta 56 (1973) 2204.
[38] C. Pretsch, S. Seibl, Tabellen zur Strukturaufklärung organischer Verbindungen mit spek-troskopischen Methoden, Vol. 3, Springer, Berlin, 1990.
[39] J. Kriwanek, Thesis, TH Leuna-Merseburg, 1984.
[40] J. Mattay, Tetrahedron 41 (1985) 2393.
[41] A. Kunze, U. Müller, K. Tittes, J.P. Fouassier, F. Morlet-Savary, J. Photochem. Photobiol. A: Chem. 110 (1997) 115.
[42] H.-J. Timpe, U. Oertel, B. Hundhammer, Z. Chem. 25 (1985) 144.